EXPERIMENTAL STUDIES ON HEAT TRANSFER AND FRICTION FACTOR CHARACTERISTICS OF A TURBULENT FLOW FOR INTERNALLY GROOVED TUBES

by

Selvaraj PONNUSAMY [a], Rajasekaran SHANMUGAM [b], Suresh SIVAN [c], and Sarangan JAGANATHAN [c]*

[a] Department of Mechanical Engineering, VIT, Ulundurpet, Tamil Nadu, India
[b] Department of Mechanical Engineering, University College of Engineering,
Villupuram, Tamil Nadu, India
[c]Department of Mechanical Engineering, NIT, Tiruchirappalli, Tamil Nadu, India

This paper reports experimental studies on friction factor, Nusselt number, and thermal hydraulic performance of a tube equipped with the classic three modified internally grooved tubes. Heat transfer and friction factor characteristics and pressure drop results have been obtained experimentally for a fully developed water flow in a grooved tube is also reported. Tests were performed for Reynolds number ranges from 5000-13500 for different geometric grooved tubes (circular, square, and rapezium). The ratio of length-to-diameter is 38.69 D. Among the grooved tubes, heat transfer enhancement obtained up to 47% for circular grooved tube, 31% for square grooved tube, and 52% for trapezoidal grooved tube in comparison with the smooth tube. It has been observed that the friction factor high in the case of square grooved tube than those of other tubes.

Key words: *friction factor, Nusselt number and square grooved tube*

Introduction

Heat transfer enhancement (HTE) techniques can the divided into two categories passive and active. In passive HTE an object which does not use external energy, such as groove inside the tube, has the duty of increasing the heat transfer rate [1, 2] An experimental investigation was carried out on heat transfer and friction factor characteristics with internally grooved tubes [3]. Forced convection heat transfer is the most frequently employed mode of the heat transfer in heat exchangers or in various chemical process plants. The use of turbulence promotes or roughness elements, such as welded ribs, grooves or wires on the surface, is a common technique to enhance the rate of heat transfer [4] use of the artificial grooved or fluted tubes is widely used in modern heat exchangers, because they are very effective in heat transfer augmentation.

Sivashanmugam and Suresh [5] investigated the heat transfer and friction factor characteristics of a circular tube fitted with a full length helical screw element with different twist ratios. They reported higher performance of helical twisted insert in comparison with the twisted

___
* Corresponding author; e-mail: selvarajgold@gmail.com

S1006

Ponnusamy, S., *et al.*: Experimental Studies on Heat Transfer and Friction Factor ...
THERMAL SCIENCE: Year 2016, Vol. 20, Suppl. 4, pp. S1005-S1015

tape insert. In continuation of this research, they studied the heat transfer augmentation and friction factor in tubes fitted with regularly spaced helical screw tape inserts [6]. Despite the high pressure drop caused by an insert in a tube using tube insert in heat exchangers has received a lot of attention during the last two decades.

Eiamsa-Ard *et al*. [7] presents the applications of a mathematical model for simulation of the swirling flow in a tube induced by loose – fit twisted tape insertion. Zimparrov [8, 9] experiments a simple mathematical model flowing, the suggestions of Smithbery and Landis has been created to predict the friction factors for the case of a fully developed turbulent flow in a spirally corrugated tube combined with a twisted tape insert. Goto *et al*. [10, 11] investigated the condensation and evaporation augmentations in internally grooved tube. The measured data yield a set of Nusselt number correlations. There were also studies examining the helically corrugated tubes [12].The corrugated tubes induce a secondary flow in a form of single vortex. Some of the studies investigating heat transfer and friction co-efficient were conducted in square coiled-wires [13]. Conical ring inserts [14]. All inserts were inserted into the tube by wall attached position, except twisted tape.

There are numerous investigations using the periodic and fully developed flow concepts on fluid flow and heat transfer for the parallel plate channels with periodically grooved parts. Promvonge [15] investigated that the snail entry with the coiled square-wire provides higher heat transfer rate than that with the circular tube of under the same conditions. The HTE can create one or more combinations of the following conditions that are favorable for the increase in heat transfer rate with an undesirable in increase in friction: (1) interruption of boundary layer development and rising degree of turbulence, (2) increase in heat transfer area, and (3) generating of swirling and/or secondary flows. To date, several studies have been focused on passive HTE methods reverse/swirl flow devices (rib, groove, wire coil, conical ring snail entry, twisted tape, winglet, *etc*.,) form an important group of passive augmentation technique [16].

Dong *et al*. [17] conducted test for air side Reynolds number in the range of 800-1500 with different fin pitches, fin lengths, and fin heights at a constant tube side water flow rate of 2.5 m³/h. Zhang *et al*. [18] experimental study on evaporation heat transfer of R 417A flowing inside horizontal smooth and two internally grooved tubes with different geometrical parameters was conducted with the mass flow rate range from 176 to 344 kg/s. Based on the experimental results, the mechanism and mass flow rate, heat flux, vapor quality and enhanced surface influencing the evaporation heat transfer coefficient were analyzed and discussed.

In the present study the pipe flow with three types of grooved tubes (circular, square, and trapezoidal) at constant wall flux condition is studied experimentally for Reynolds number ranges from 5000-13500 and groove depth was fixed to investigate the effect of the groove shapes on heat transfer. The experimental results are compared to that of the smooth tube to obtain the heat transfer and pressure drop are reported to reveal experimentally efficient pipe groove configurations. The thermal hydraulic performance for all the cases was also performed.

Experimental set-up and procedure

The experimental set-up and schematic diagram of the experimental apparatus are shown in figs. 1 and 2, respectively. The open test loop consists of a reservoir, centrifugal pump, calming section, test sections (plain tube, circular, square, and trapezoidal grooved tubes), riser section, and collecting tank. Water was used as test fluid. The pump used in this work was a centrifugal type, in which the flow rate controlled by the rotational speed. Water was driven by the pump from reservoir to flow through the test section. The plain carbon steel tube with hydrodynamic development section of length 2140 mm, the test section length of 1700 mm with

Ponnusamy, S., *et al.*: Experimental Studies on Heat Transfer and Friction Factor ...
THERMAL SCIENCE: Year 2016, Vol. 20, Suppl. 4, pp. S1005-S1015

S1007

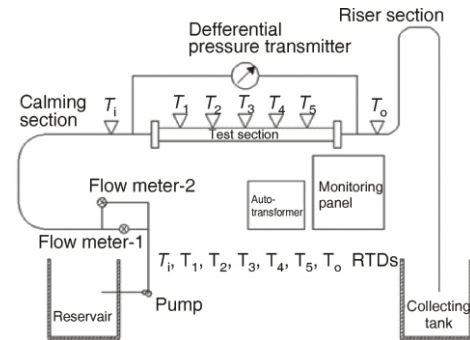**Figure 1. Experimental set-up**

Figure 2. Schematic diagram of the experimental apparatus

38.14 mm inner diameter, and 48.26 mm outer diameter was used for experiment. The test section is first wound with sun mica to isolate it electrically. Then ceramic beads coated electrical SWG Nichrome heating wire giving maximum power of 3000 W is wounded over it. Over the electrical windings, the test sections with thick insulation consisting of layer of ceramic fiber, asbestos rope, glass wool another layer of asbestos rope at the outer surface is provided to prevent the radial heat loss. The test section is isolated thermally from its upstream and downstream by plastic bushings to minimize the heat loss resulting from axial heat conduction. The terminals of the heating coils were connected to the auto-transformer with 3 kW capacities, by which the heat flux can be varied by varying the voltage. Five calibrated RTD PT 100 type temperature sensors of 0.1 °C accuracy with digital indicator were placed along the test tube in line with 250 mm spacing each other for measuring the outside wall temperatures of test sections. The inlet and outlet temperature, T_i and T_o, respectively, measured by two RTD PT 100 type temperature sensors immersed in the mixing chambers provided at inlet and outlet. A differential pressure transmitter able to read up to 1 cm of water is mounted across the test section to measure the pressure drop. Calibrated flow meter having range 6 lpm to 22 lpm is used for measurement turbulent flow. Digital monitoring panel displays the reading of pressure drop, flow rates and wall temperature variations of the test section. Proper care was taken to prevent the leakage in all parts of the experimental set-up.

The sectional view of the test section and grooved tubes and geometric shapes of grooved tubes are shown in figs. 3 and 4, respectively.

Experimental procedure

The centrifugal pump was switched on, and the water flow rate to the test section was adjusted using by-pass valve. A sufficient time of 15 minutes were allowed to obtain a steady-state. The heat flux was set by adjusting the electrical voltage with the help of auto-transformer, and the constant heat flux was allowed to continue till the steady-state was reached. The steady-state was obtained within one hour for the
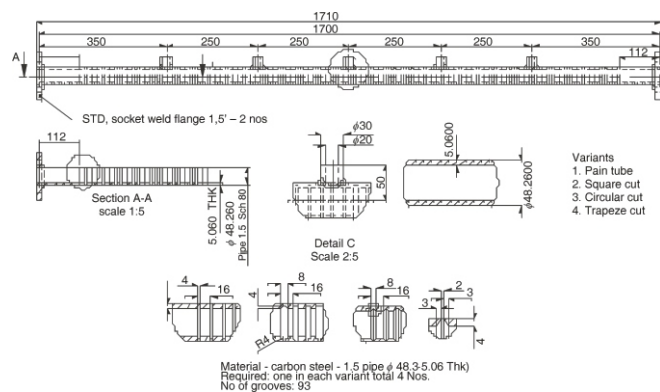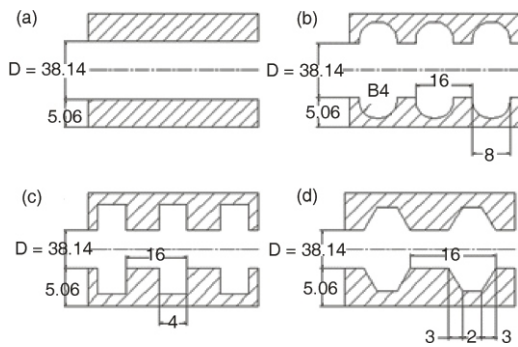

Figure 3. Sectional view of the test section and grooved tubes (plain, circular, square, and trapezoidal grooves)

Figure 4. Geometric shape of the grooved tubes in mm;
(a) plain tube, (b) circular groove, (c) square groove, and (d) trapezoidal groove

first run and 25 minutes for the subsequent runs. The inlet and outlet temperature of water and the wall temperatures in all RTD temperature sensors were recorded after steady-state is reached. The electrical heat flux was measured by calibrated ammeter and voltmeter and also with the help of wattmeter. The flow rates to the test section and heat flux were varied and readings were taken after attaining steady-state. The experiments were conducted for plain tube, and subsequently circular, square and trapezoidal grooved tubes. The pressure drop was measured for each flow rate with the help of digital pressure transmitter under isothermal condition of flow.

Data reduction

The net heat transfer rate from the inner tube surface to the fluid flow passing through the test tube by convection can be calculated subtracting heat losses from the total electrical power input at the steady-state conditions, Tanda [19], Wang and Sunden [20, 21], Chang *et al.* [22], and Bilen *et al.* [3]. The net rate heat transfer is also equal to the rate of the heat transfer given to the fluid passing through the test section, using inlet and outlet temperature difference and mass flow rate Zimparov [12] Vicente *et al.* [1], and Rahimi *et al.* [2], the energy balance equation can be written:

$$q_{net} = q_{vol} - q_{loss} = mC_p(T_o - T_i) \tag{1}$$

were q_{net} is the net heat transfer rate given to the fluid inside the test tube, q_{vol} – the measured electrical power input to the heater, q_{loss} denotes all the heat losses from the test section.

On the other hand, the heat transfer may be approximated by:

$$q_{net} = hA(T_w - T_b)$$

where

$$T_b = \frac{(T_0 + T_i)}{2} \text{ and } T_w = \frac{\Sigma T_w}{5} \tag{2}$$

Using eqs. (1) and (2) the convection heat transfer coefficient on the grooved tube wall at the steady-state can be calculated by:

$$h = \frac{mC_p(T_o - T_i)}{A(T_w - T_b)} \tag{3}$$

where A is the inner surface area of the plain tube, T_o and T_i – the outlet and inlet temperature of water flow, respectively, T_w – the average wall temperature. The average Nusselt number is calculated as:

$$Nu = \frac{hD}{k} \tag{4}$$

The Reynolds number is based on the flow velocity and the tube inlet diameter and is given by:

$$Re = \frac{VD}{\nu} \tag{5}$$

The friction factor can be determined by measuring the pressure drop across the test tube length:

$$f = \frac{\Delta P}{\left(\dfrac{L}{D}\right)\left[\rho\left(\dfrac{V^2}{2}\right)\right]}$$

(6)

where ΔP is the pressure drop across the test tube measured by an electronic pressure transmitter, L – the test tube length, V – the mean water velocity at the entrance of the test section which was calculated from volumetric flow rate divided by the cross-section area of the tube, and D – the inner diameter of the test tube. The thermo physical properties of water was evaluated at the bulk fluid temperature $T_b = (T_0 + T_i)/2$:

– Prandtl number
$$\mathrm{Pr} = \frac{C_p \mu}{k}$$
(7)

– area of cross-section
$$a = \frac{\pi}{4} D^2$$
(8)

– kinematic viscosity
$$v = \frac{\mu}{\rho}$$
(9)

– mass flow rate
$$m = \rho A V$$
(10)

– effectiveness
$$\frac{\mathrm{Nu}}{\mathrm{Nu}_0}$$
(11)

The thermal performance for evaluating the increased heat transfer is based on the same area and pumping power. The following expression which was suggested by Park *et al.* [23] is then used:

thermal hydraulic performance
$$\eta = \left(\frac{\dfrac{\mathrm{Nu}}{\mathrm{Nu}_0}}{\sqrt[3]{\dfrac{f}{f_0}}}\right)$$
(12)

where Nu_0 and f_0 are Nusselt number and friction factor for a plain tube, respectively.

The physical properties of water are taken from data book, Kothandaraman and Subramanian [24]. The SI unit conversion reference in Soman [25] = handbook. Microsoft excel worksheet was used to calculate Reynolds number, Nusselt number, friction factor, effectiveness of the grooved tubes, and thermal hydraulic performance of the grooved tubes. The ASHRAE data and experimental values match nicely (maximum difference of ±4%) with temperature ranging from 29 °C to 36 °C.

Experimental uncertainty was calculated following Coleman and Steele [26] and ANSI/ASME [27] standard. The uncertainties associated with the experimental data are calculated on the basis 95% confidence level. The measurement uncertainties used in the method are: bulk fluid temperature and wall temperatures ±0.1 °C, fluid flow rate ±2%, and fluid properties ±2%. The uncertainty calculation showed that a maximum of ±1%, ±2%, and ±1.7% for Reynolds number, friction factor, and Nusselt number, respectively. Cai *et al.* [29] in the design, most commonly, correlations are developed in terms of dimensionless groups like the Nusselt, Reynolds, and Prandtl numbers; sometimes for greater generality geometrical factors are also included. Assuming a functional relationship between the groups with a certain number of free constants, a regression analysis to minimize the error between predicted and experimental val-

ues is carried out to determine the appropriate value of constants. The heat transfer correlations that can be used to predict the performance of thermal components.

Results and discussion

Validation of the experimental data for the smooth tube

The present experimental results on heat transfer and friction factor characteristics in a plain tube are first validated in terms of Nusselt number and friction factor. The Nusselt number and friction factor obtained from plain tube are compared with the correlations of Gnielinski and Petukhov [29] found in the open literature for turbulent flow in circular tubes is:

$$\text{Nu} = \frac{\left(\dfrac{f}{8}\right)(\text{Re}-100)\,\text{Pr}}{1+12.7\sqrt{\dfrac{f}{8}}\,(\sqrt[3]{\text{Pr}^2}-1)} \qquad \text{for Re} > 3000 \tag{13}$$

where

$$f = \frac{1}{(0.790\,\ln \text{Re}-1.64)^2}$$

The Nusselt number for plain tube is given by the Dittus and Boelter [30] correlation for a fully developed region:

$$\text{Nu} = 0.023\,\text{Re}^{0.8}\,\text{Pr}^{0.4} \quad \text{for} \quad \text{Re} \geq 10.000 \tag{14}$$
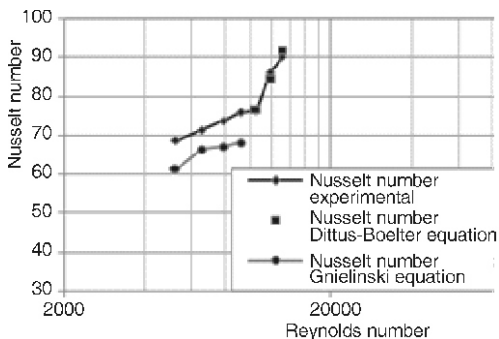

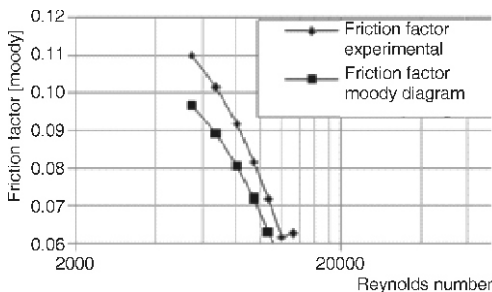**Figure 5. Nusselt number *vs.* Reynolds number for smooth tube**

Figure 6. Verification (b) friction factor *vs.* Reynolds number for the smooth tube

The friction factor for a smooth tube is by the friction factor correlations from Moody [31] is of the form:

$$f = 0.316\,\text{Re}^{-0.25} \quad \text{for} \quad \text{Re} \leq 2\cdot10^4 \tag{15}$$

The comparison of the experimental and estimated values of the Nusselt number and friction factor as a function of the Reynolds number is shown in figs. 5 and 6, respectively. The average deviation of the experimental values of the Nusselt number is 8% from the values predicted by eq. (13) and 2% by eq. (14) and average deviation of the experimental values of the measured friction factor is 12% from the values predicted by eq. (15). Thus reasonable good agreement between the two sets of values ensures the accuracy of the data being collected with the experimental set-up.

Grooved pipe results

The variation of Nusselt number with Reynolds number for plain tube and grooved tubes is shown in fig. 7. By referring the figure one can observe that as Reynolds number increases, Nusselt number increases. The overall

Ponnusamy, S., *et al.*: Experimental Studies on Heat Transfer and Friction Factor ...
THERMAL SCIENCE: Year 2016, Vol. 20, Suppl. 4, pp. S1005-S1015

S1011

results show that in all setups, the Nusselt numbers were higher than those obtained for plain tube. The figure shows that highest Nusselt numbers were obtained in a trapezoidal grooved tube and lowest Nusselt numbers for square grooved tube among the grooved tubes. As seen from fig. 7 heat transfer is quit close to each other for circular and trapezoidal grooves (Nusselt number values are closes to each other). It is observed that more increase in the heat transfer augmentation for grooved tubes due to flow mixing and disturbance than that of plain tube. It can be said that thermal boundary layers for grooved flow became thinner than the case of plain tube and secondary vortices inside the grooves contributed to the enhancement of the heat transfer.

Figure 7. Nusselt number *vs*. Reynolds number for various grooved tubes

The measured friction factors for the grooved tubes significantly are higher than that obtained for the plain tube. For all the arrangements, it is found that the friction factor values were higher at lower Reynolds number. Also, the measured friction factors of the trapezoidal grooved tube and circular grooved tube nearly same values for all the constant heat flux observations. But, the square grooved tube friction factor is minimum, when compared with grooved tubes. For the plain and grooved tubes, the variation of the measured values of friction factor with Reynolds numbers is shown in fig. 8. It shows that the friction factor decreases with increase of Reynolds number. By using grooved tubes the maximum friction factor were obtained up to 73% for circular grooved tube, 50% for square grooved tube, and 78% for trapezoidal grooved tube more than plain tube. Bilen *et al*. [3] the circular and trapezoidal grooves can reduce the occurrence of the flow re-circulation providing more surface sweep, therefore negative effect of the re-circulation region on the heat transfer can be decreased by avoiding.

Figure 8. Friction factor *vs*. Reynolds number for various grooved tubes sharp vertical corner of the groove; for the square grooved tube, less increase in heat transfer can be explained by the occurrence of the flow re-circulation region inside the groove

The effectiveness of heat transfer augmentation for grooved tubes to that of plain tube was compared in fig. 9. It is seen that for the entire grooved tube cases heat transfer ratio increased in comparison with the plain tube. Among the grooved tubes, effectiveness of circular and trapezoidal grooved tube is nearly same for most of the observations when compared with square grooved tube. The HTE was obtained up to 52%, 32%, and 54% for circular, square, and
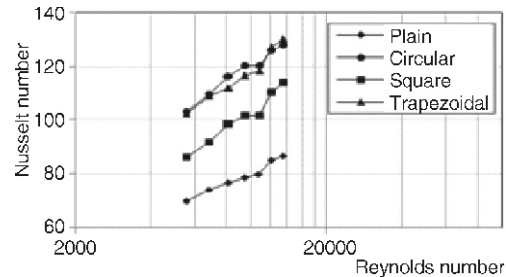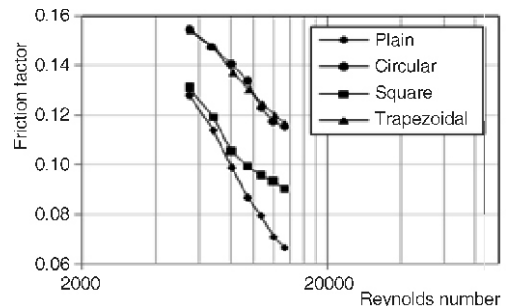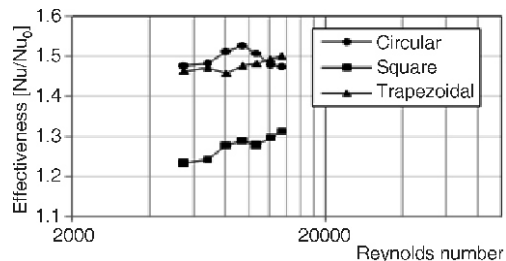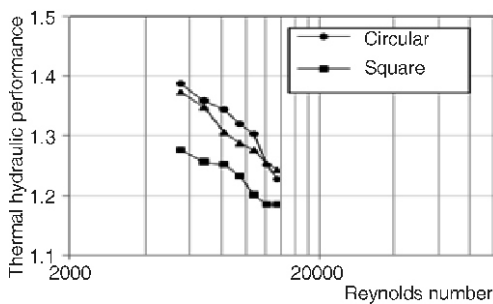

Figure 9. Nu/Nu_0 *vs*. reynolds number for various grooved tubes

trapezoidal grooved tubes, respectively. Bilen *et al*. [3] experimentally investigated the heat transfer characteristics with number of grooves same for circular and rectangular grooves, less number of grooves for trapezoidal grooved tube and air is used as working fluid. Promvonge [15] used a coiled wire for the experiment and provides considerable heat transfer augmentations; Nu/Nu_0 = 1.8-2.6. His another experiment, used coiled wires with snail entry causes a high pressure drop and also provides considerable heat transfer augmentations; Nu/Nu_0 = 3.4-3.9. The literature explains that the effectiveness decreases with the increase of Reynolds numbers.

Figure 10. The performance ratio *vs*. Reynolds number for various grooved tubes

The thermal hydraulic performances of grooved tubes are shown in fig. 10. It shows that the present grooved tubes provide higher heat transfer performance than the plain tube. The trapezoidal grooved tube consistently possesses the higher thermal performance than those of circular and square grooved tubes. Further, a close inspection reveals that thermal performance both trapezoidal grooved tube and circular grooved tube having slight variation. The performance increases is due to only the fluid mixing because of having same number of grooves and pitch. The thermal hydraulic performance in terms of η is illustrated in fig. 10. These types of plots may be helpful to choose the working range so as to provide $\eta \geq 1$. The working conditions should satisfy $\eta \geq 1$. It is seen from the figures that thermal hydraulic performance tends to decrease as Reynolds number increases for all cases. As can be seen in the figures that heat transfer performance is greater than unity ($\eta \geq 1$) for all the present grooves.

As indicated in the present work pitch, length, depth, and number of grooves of all the grooved tubes (circular, square and trapezoidal) are same and water is used for working fluid. Bilen *et al*. [3] experimentally investigated the heat transfer characteristics with number of grooves same for circular and rectangular grooves, less number of grooves for trapezoidal grooved tube and air is used as working fluid.

Correlations of Nusselt number and friction factor

Using the data obtained from experiment, the average Nusselt numbers and friction factors for both plain and grooved tubes were correlated as a function of Reynolds number. The correlations proposed for Nusselt number and friction factor for plain and grooved tube are:

$$Nu = 3.72 \, Re^{0.416} \, Pr^{-0.431} \tag{16}$$

$$f = 1.152 \, Re^{-0.279} \tag{17}$$

$$Nu = 95.2 \, Re^{0.291} \, Pr^{-1.41} \tag{18}$$

$$f = 1.009 \, Re^{-0.222} \tag{19}$$

For square grooved tubes:

$$Nu = 79.43 \, Re^{0.282} \, Pr^{-1.35} \tag{20}$$

Ponnusamy, S., *et al.*: Experimental Studies on Heat Transfer and Friction Factor ...
THERMAL SCIENCE: Year 2016, Vol. 20, Suppl. 4, pp. S1005-S1015

S1013

$$f = 1.014\,\mathrm{Re}^{-0.252} \tag{21}$$

For trapezoidal grooved tubes:

$$\mathrm{Nu} = 0.287\,\mathrm{Re}^{0.497}\,\mathrm{Pr}^{0.848} \tag{22}$$

$$f = 1.015\,\mathrm{Re}^{-0.223} \tag{23}$$

The mean deviations of the predicted Nusselt number for plain, circular, square, and trapezoidal grooved tubes are 1%; and the corresponding maximum deviations are 9%, 2%, 5%, and 9%, respectively. The mean deviations of the predicted friction factor for the grooved tubes 1%, 1.07%, and 1%; and the corresponding maximum deviations are 5%, 3%, and 4%, respectively.

The predicted value of Nusselt number by eqs. (16), (18), (20), and (22) for plain, circular, square, and trapezoidal grooved tubes compared with experimental values are shown in fig. 11. The predicted value of friction factor by eqs. (17), (19), (21), and (23) for plain, circular, square, and trapezoidal grooved tubes compared with experimental values are shown in fig. 12.
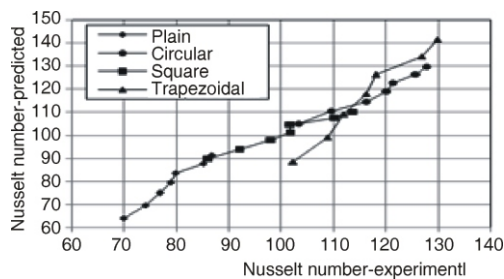
Figure 11. Comparison between predicted and experimental data for Nusselt number for plain and grooved tubes
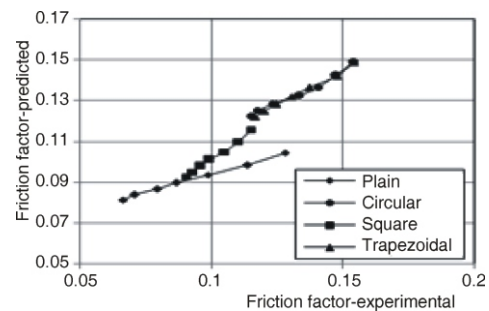
Figure 12. Comparison between predicted and experimental data for friction factor number for plain and grooved tubes

Conclusions

The effects of various grooved tubes on the heat transfer and friction characteristics were experimentally investigated for turbulent flow. The thermal performances were used to evaluate the effectiveness of the grooved tubes. The results of the present work can be summarized.

- The heat transfer rate increases with increasing Reynolds number for all the grooves due to thinner of boundary layer.
- The variation of friction factors for all grooved tubes tends to be closer to each other in the considered range of Reynolds number and it is seen that friction factor is almost independent of Reynolds number.
- The comparison between plain and grooved tubes results show that the heat transfer augmentation is due to only fluid mixing and disturbances that occur in grooved tubes.
- Nusselt number and friction factor for each grooved tube and plain tube were correlated as a function of Reynolds number for both laminar and turbulent flow.
- The maximum thermal hydraulic performance for circular, square, and trapezoidal grooved tubes are 47%, 31%, and 52%, respectively in the case of laminar flow.
- For turbulent flow the grooved tubes, maximum performance is obtained up to 38% for circular grooved tube, 27% for square grooved tube, and 40% for trapezoidal grooved tube in comparison with plain tube.

• That the flow disturbances and higher intensity turbulence of the water close to the tube wall can be one of the reasons that highest performance obtained by trapezoidal grooved tube.

Nomenclature

A	– heat transfer surface area, [m^2]	Re	– Reynolds number ($=VD/\nu$)
C_p	– specific heat capacity, [kJkg^{-1}K^{-1}]	T	– temperature, [K]
D	– inner diameter of test tube, [m]	V	– mean velocity at the inlet of the tube, [ms^{-1}]
f	– friction factor		
h	– convective heat transfer coefficient, [Wm^{-2}k^{-1}]	*Greek symbols*	
k	– thermal conductivity of water, [Wm^{-1}k^{-1}]	η	– thermal hydraulic performance
L	– length of test tube, [m]	ν	– kinematics viscosity, [m^{2}s^{-1}]
m	– mass flow rate of water, [kgs^{-1}]	ρ	– density of water, [kgm^{-3}]
Nu	– Nusselt number ($=h\,D/k$)		
Pr	– Prandtl number ($=\mu C_p/K$)	*Subscripts*	
ΔP	– pressure difference, [Nm^{-2}]	b	– mean
q_{loss}	– loss of heat transfer	i	– inlet
q_{net}	– net heat transfer	o	– outlet
q_{vol}	– electrical power input	w	– local wall
		0	– plain tube

References

[1] Vincente, P. G., *et al.*, Experimental Investigation on Heat Transfer and Frictional Characteristics of Spirally Corrugated Tubes in Turbulent Flow at Different Prandtl Numbers, *Int. J. Heat Mass Transfer, 47* (2004), 1, pp. 671-681

[2] Rahimi, M., *et al.*, Experimental and CFD Studies on Heat Transfer and Friction Factor Characteristics of a Tube Equipped with Modified Twisted Tape Insert, *Int. J. Chemical Engineering and Processing, 48* (2009), 3, pp. 762-770

[3] Bilen, K., *et al.*, The Investigation of Groove Geometry Effect on Heat Transfer for Internally Grooved Tubes, *Int. J. Applied Thermal Engineering, 29* (2009), 4, pp. 753-761

[4] Karwa, R., *et al.*, Heat Transfer Coefficient and Friction Factor Correlations for the Transitional Flow Regions in Rib – Roughened Rectangular Ducts, *Int. J. Heat Mass Transfer, 42* (1999), 9, pp. 1597-1615

[5] Sivashanmugam, P., Suresh, S., Experimental Studies on Heat Transfer and Friction Factor Characteristics of a Laminar Flow through a Circular Tube Fitted with Helical Screw-Tape Inserts, *Applied Thermal Engineering, 26* (2006), 16, pp. 1990-1997

[6] Sivashanmugam, P., Suresh, S., Experimental Studies on Heat Transfer and friction Factor Characteristics of a Turbulent Flow Through a Circular Tube Fitted with Regularly Spaced Helical Screw-Tape Inserts, *Int. J. Applied Thermal Engineering, 27* (2007), 8-9, pp. 1311-1319

[7] Eiamsa-Ard, S., *et al.*, 3-D Numerical Simulation of Swirling Flow and Convective Heat Transfer in a Circular Tube Induced by Means of Loose Fit Twisted Tapes, *Int. J. Communications in Heat Mass Transfer, 36* (2009), 9, pp. 947-955

[8] Zimparov, V., Prediction of Friction Factors and Heat Transfer Coefficient for Turbulent Flow in Corrugated Tubes Combined with Twisted Tape Inserts, Part 1: Friction Factors, *Int. J. Heat and Mass Transfer, 47* (2004), 3, pp. 589-599

[9] Zimparov, V., Prediction of Friction Factors and Heat Transfer Coefficients for Turbulent Flow in Corrugated Tubes Combined with Twisted Tape Inserts, Part 2: Heat Transfer Coefficients, *Int. J. of Heat and Mass Transfer, 47* (2004), 2, pp. 385-393

[10] Goto, M., *et al.*, Condensation and Evaporation Heat Transfer of R410A Inside Internally Grooved Horizontal Tubes, *Int. J. Refrigeration, 24* (2001), 7, pp. 628-638

[11] Goto, M., *et al.*, Condensation Heat Transfer of R410A Inside Internally Grooved Horizontal Tubes, *Int. J. Refrigeration, 26* (2003), 4, pp. 410-416

[12] Zimparov, V., Enhancement of Heat Transfer by a Combination of Three Start Spirally Corrugated Tubes with a Twisted Tape, *Int. J. Heat Transfer, 44* (2001), 3, pp 551-574

[13] Promvonge, P., Heat Transfer Behaviors in Round Tube with Conical Ring Inserts, *Energy Conversion Management, 49* (2008), 1, pp. 8-15

Ponnusamy, S., *et al.*: Experimental Studies on Heat Transfer and Friction Factor ...
THERMAL SCIENCE: Year 2016, Vol. 20, Suppl. 4, pp. S1005-S1015

S1015

[14] Promvonge, P., Thermal Enhancement in a Round Tube with Snail Entry and Coiled – Wire Inserts, *Int. J. International Communications in Heat and Mass Transfer, 35* (2008), 5, pp. 623-629

[15] Promvonge, P., Thermal Augmentation in Circular Tube with Twisted Tape and Wire Coil Turbulators, *Int. J. Energy Conversion and Management, 49* (2008), 11, pp. 2949-2955

[16] Promnvonge, P., Thermal Performance in Circular Tubes Fitted with Coiled Square Wires, *Energy Conversion Management, 49* (2008), 5, pp. 980-987

[17] Dong, J., *et al.*, Heat Transfer and Pressure Drop Correlations for the Wavy Fin and Flat Tube Heat Exchangers, *Int. J. Applied Thermal Engineering, 27* (2007), 11-12, pp. 2066-2073

[18] Zhang, X., *et al.*, Heat Transfer Characteristics for Evaporation of R417A Flowing Inside Horizontal Smooth and Internally Grooved Tubes, *Int. J. Energy Conversion and Management, 49* (2008), 6, pp. 1731-1739

[19] Tanda, G., Heat Transfer in Rectangular Channels with Transverse and v-Shaped Broken Ribs, *Int. J. Heat and Mass Transfer, 47* (2004), 2, pp. 229-243

[20] Wang, L., Sunden, B., Performance Comparison of Some Tube Inserts, *Int. J. Communications in Heat and Mass Transfer, 29* (2002), 1, pp. 45-46

[21] Wang, L., Sunden, B., Experimental Investigation of Local Heat Transfer in a Square Duct with Various Shaped Ribs, *Int. J. Heat and Mass Transfer, 43* (2007), June, pp. 759-766

[22] Chang, S. W., *et al.*, Heat Transfer and Pressure Drop in Tube with Broken Twisted Tape Insert, *Int. J. Experimental Thermal and Fluid Science, 32* (2007), 2, pp. 489-501

[23] Park, J. C., *et al.*, Heat Transfer Performance of Five Different Rectangular Channels with Parallel Angled Ribs, *Int. J. Heat and Mass Transfer, 35* (1992), 11, pp. 2891-2903

[24] Kothandaraman, C. P., Subramaniyan, S., *Heat and Mass Transfer Data Book*, New Age International Publishers, New Delhi, India, 2010

[25] Soman, K., International System of Units, A Handbook on SI Units for Scientists and Engineers, 2nd Printing, PHI Learning, New Delhi, 2010

[26] Coleman, H. W., Steele, W. G., Experimental and Uncertainty Analysis for Engineers, John Wiley and Sons, New York, USA, 1989

[27] ***, ANSI/ASME, 1986, Measurement Uncertainty, PTC. 19.1-1985, 1986

[28] Cai, W., *et al.*, Heat Transfer Correlations by Symbolic Regression, *Int. J. Heat and Mass Transfer, 49* (2006), 23-24, pp. 4352-4359

[29] Petukhov, B. S., Heat Transfer and Friction in Turbulent Pipe Flow with Variable Physical Properties in: Advances in Heat Transfer, Academic Press, New York, USA, Vol. 6, 1976, pp. 503-564

[30] Dittus, F. W., Boelter, L. M. K., *Heat Transfer in Automobile Radiators of the Tubular Type*, University of California Press, Berkerely, Cal., USA, Vol., 2 1930, pp. 443-461

[31] Moody, L. F., Friction Factors for Pipe Flow, *Trans. Asme, 66* (1944), 67, pp. 1-684